

General Disclaimer

One or more of the Following Statements may affect this Document

- This document has been reproduced from the best copy furnished by the organizational source. It is being released in the interest of making available as much information as possible.
- This document may contain data, which exceeds the sheet parameters. It was furnished in this condition by the organizational source and is the best copy available.
- This document may contain tone-on-tone or color graphs, charts and/or pictures, which have been reproduced in black and white.
- This document is paginated as submitted by the original source.
- Portions of this document are not fully legible due to the historical nature of some of the material. However, it is the best reproduction available from the original submission.

X-625-71-154
PREPRINT

NASA TM X- 65552

THEORY OF THE 24.5/73.6 MHz CW PROPAGATION EXPERIMENT

JOHN E. JACKSON

APRIL 1971



GSFC

GODDARD SPACE FLIGHT CENTER
GREENBELT, MARYLAND

N71-27670

(ACCESSION NUMBER)

28
(PAGES)

TMX-65552
(NASA CR OR TMX OR AD NUMBER)

G3

(CODE)

07

(CATEGORY)

FACILITY FORM 602

THEORY OF THE 24.5/73.6 MHz CW PROPAGATION EXPERIMENT

by

John E. Jackson
Laboratory for Planetary Atmospheres
NASA/Goddard Space Flight Center
Greenbelt, Maryland

ABSTRACT

This report presents an improved theoretical treatment of the two-frequency (24.5/73.6 MHz) rocket-to-ground CW propagation experiment for in situ electron density measurements. The propagation experiment measures the difference between two phase path integrals, and the local electron density is calculated from the rate of change of this difference. The basic relationships are derived directly from the concept of equivalent vertical electron content. This leads to formulas in which temporal and spatial ionospheric variations appear in explicit form. These variations give rise to errors, which depend upon both fluctuation rates and geometric factors associated with the rocket trajectory. Examples of these errors are given for typical experimental conditions.

INTRODUCTION

Seddon's two-frequency CW propagation experiment (Ref. 1) has been used extensively for rocket measurements of ionospheric electron density distributions. Basically, the experiment consists in phase path measurements accomplished by transmitting two CW signals from a moving rocket to receiving and recording stations on the ground. A suitable low frequency was selected to obtain the ionospheric data and its 6th harmonic was used for comparison purposes. The experiment provides the difference between the high - and the low-frequency phase paths as a function of time (or equivalently altitude) from which the vertical electron density distribution can be computed. The 6-to-1 frequency ratio was used for the experiments conducted from 1946 to 1961. The lower of the two frequencies, initially 4.27 MHz, (1946) was changed to 7.75 MHz in 1954 and to 12.27 MHz in 1959. Since 1962 the experiment has been conducted primarily at 24.5 and 73.6 MHz using a 3-to-1 frequency ratio. The 24.5/73.6 MHz experiment has been performed on 8 rocket flights from Wallops Island, Va. (Ref. 2, 3 and 4), on 6 rocket flights from a shipboard launcher near the coast of Peru (Ref. 5), and on 3 rocket flights from Thumba, India (to be published).

A general theory of the experiment which is applicable to the relatively low frequencies (4.27 and 7.75 MHz) used by Seddon has been described by Jackson (Ref. 6). At 24.5

and 73.6 MHz the formulas given by Jackson (Ref. 6) can be simplified as shown by Bauer and Jackson (Ref. 2).

It was realized in previous treatments that the analysis yields an error term which arises from time variations in the ionosphere, and which affects the accuracy of the measurements primarily near the peak of the rocket trajectory. This has led to the conclusion that the measurements are usually reliable up to an altitude within 5-to-10 km of apogee. Below these altitudes the accuracy of the measurements was estimated to be about 5 per cent. The present treatment re-examines this question in much greater detail than had previously been done. The present analysis starts with basic principles but takes immediate advantage of the simplifications which can be made at 24.5 MHz. This makes it possible to express the observations directly in terms of the electron density distribution, and to provide (at least to non-specialists) a clearer insight into the physical significance of the measurements. The present treatment retains the error term and provides an estimate of its magnitude as a function of rocket altitude.

Phase Path Concept

A CW signal propagating from A to O (both points assumed to be stationary) will (if the path $r = OA$ is in free space) experience a phase shift Ψ given by:

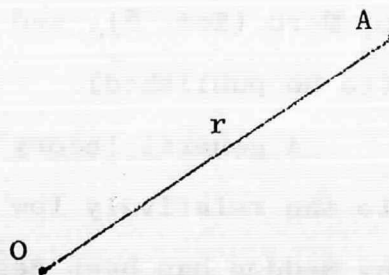


Fig. 1. Propagation path between two fixed points O and A in free space.

$$\Psi = \frac{r}{\lambda} = r \frac{f}{c} \text{ cycles} \quad (1)$$

where:

r = distance OA in km

λ = wave length in km

f = frequency in cycles/sec.

c = velocity of light in vacuo (km/sec)

In the ionosphere the phase velocity v_p is:

$$v_p = \frac{c}{n}$$

where:

n = refractive index = $F(\frac{N}{f^2}, B, \phi)$

and,

N = electron density (electrons/cm³),

B = induction (gauss) of terrestrial magnetic field,

ϕ = angle between \vec{B} and direction of propagation.

The parameter B causes the refractive index to be double-valued and this gives rise to two modes of propagation. The present discussion assumes that we are dealing with only one of these two modes. A more complete treatment will be given later in the Appendix.

For the 24.5 MHz experiment, ray bending effects can be neglected and we can also assume that the direction of phase propagation coincides with the direction of energy propagation. In other words we can assume that the wave is still propagating along AO, even if part of the path is within the ionosphere. The phase shift $\Delta\Psi$ for an interval Δr is:

$$\Delta\Psi = \Delta r \frac{f}{v_p} = \frac{f}{c} n \Delta r \text{ cycles} \quad (2)$$

and the total phase shift is therefore:

$$\Psi = \frac{f}{c} \int_0^r n(r) dr \quad \text{cycles} \quad (3)$$

The integral $\int_0^r n(r) dr$, which is known as the phase path P , represents the distance r multiplied by an average index \bar{n} as seen by Eq. (4):

$$P = \int_0^r n(r) dr = \bar{n} \int_0^r dr = \bar{n}r \quad (4)$$

CW Propagation Experiment (Basic Principles)

The CW propagation experiment provides basically a measurement (as a function of time or equivalently r) of the difference between the high- and the low frequency phase paths, i.e:

$$\begin{aligned} P_H - P_L &= \int_0^r n_H(r) dr - \int_0^r n_L(r) dr \\ &= \int_0^r (n_H - n_L) dr \end{aligned} \quad (5)$$

where the subscript H refers to the higher frequency wave and the subscript L refers to the lower frequency wave.

It should also be understood that n_H and n_L are both functions of r . For the frequencies under consideration (24.5 and 73.6 MHz) we can write (for $N < 10^6$ el/cc)

$$n_H - n_L = k N \quad (6)$$

where k is a constant.

Although Eq. (6) is very nearly correct it is not used in the actual data analysis which takes into consideration both propagation modes and uses the exact relationship between phases indices and electron density. The actual procedure used to analyze the data is described in the appendix where it is shown that the formulas derived in the text require a minor modification when N is greater than 3×10^5 el/cc.

Substituting Eq. (6) into Eq. (5) yields:

$$P_H - P_L = \int_0^r k N dr = k \int_0^r N dr$$

The CW propagation experiment (at 24.5 MHz) can therefore be viewed as yielding directly the quantity $\int_0^r N dr$, which is the total electron content from 0 to r (i.e. between points O and A of Fig. 1). The measured quantity $U(r)$ will be defined for convenience as:

$$U(r) = \frac{1}{k} (P_H - P_L)$$

Thus

$$\int_0^r N dr = U(r) \quad (7)$$

where $U(r)$ is the measurement provided by the CW propagation experiment.

A knowledge of $U(r)$ as a function of time makes it possible to derive the electron density as a function of r

(or equivalently the altitude z) as will be shown in the following sections.

Theory of experiment for $\theta = \text{Constant}$

Let point A in Fig. 1 represent the rocket-borne CW transmitter at a time t , and point O represents the receiving site on the ground. We now let A move to a position A' as shown in Fig. 2a. We will assume that the motion is in the direction of OA, i.e. that the zenith angle θ of the rocket position vector is constant. Let $AA' = \Delta r$ and let Δt represent the time interval corresponding to Δr . One example of the electron density N as a function of r is given in Fig. 2b.

When the rocket is at point A ($OA = r$), the measurement indicated by Eq. (7) represents the cross-hatched area in Fig. 2b. Repeating the measurement when the rocket is at A' ($OA' = r + \Delta r$), and subtracting the previous measurement gives:

$$\begin{aligned} U(r+\Delta r) - U(r) &= \text{area MQRS} \\ &= \Delta r(N_{av}) \end{aligned}$$

where N_{av} is the average density in the interval Δr . Thus

$$N_{av} = [U(r+\Delta r) - U(r)]/\Delta r$$

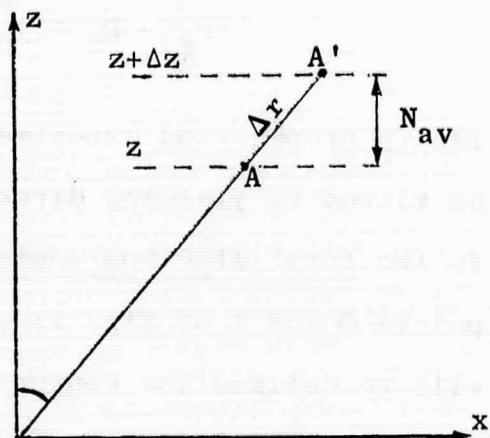


Fig. 2a. Geometry of experiment for $\theta = \text{constant}$.

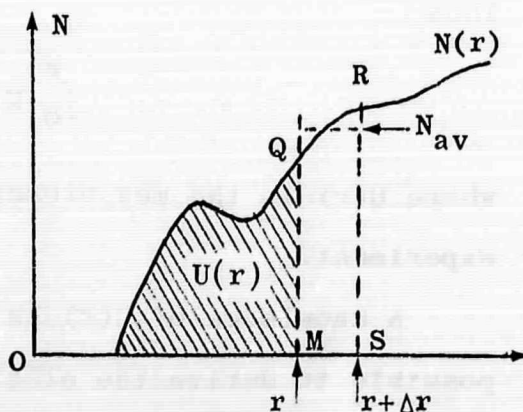


Fig. 2b. Electron density vs. r .

The above analysis (based upon a constant angle θ) also assumes that $U(r)$ has not changed in value during the time interval Δt (corresponding to Δr), i.e. it was assumed that U is a function of r only. The quantity N_{av} as defined above represents also the average density for the height interval $(z, z + \Delta z)$. The more general theory which does not assume that θ is constant leads to a formula containing the expression:

$$[U(r+\Delta r) - U(r)]/\Delta r,$$

as well as other terms. It is therefore convenient to let

$$N' = [U(r+\Delta r) - U(r)]/\Delta r \quad (8)$$

where N' represents the apparent density, i.e. the density corresponding to the assumptions:

$$\theta = \text{constant}; \text{ and } U(r, t + \Delta t) = U(r, t)$$

The assumption $\theta = \text{constant}$ holds for most of the rocket ascent, because the rocket motion is then essentially radial with respect to the launch site (and with respect to the near-by receiving site). The second assumption implies that the CW propagation experiment will yield most accurate results under quiet undisturbed ionospheric conditions. Ideal conditions for the measurements would be for the density to be a function of z only, i.e. independent of x (horizontal displacement) and t . Previous treatments of the subject have essentially assumed that the ideal conditions were fairly well approximated (during most of the ascent) by a

steep rocket trajectory, which permits the measurements to be made in a relatively short time (typically 5 minutes) and with a relatively small x displacement (typically less than 100 km). The treatment for a horizontally stratified ionosphere will be repeated here, using a more direct mathematical procedure than was previously employed.

The concept of horizontal stratification is useful as a first order approximation to the actual situation for an undisturbed ionosphere. The general formula will therefore include first order terms corresponding to horizontal stratification and second order terms arising from departures from horizontal stratification. It will then be shown that the second order terms have a negligible or very small effect during most of the rocket ascent, and that they can again have a fairly small effect over large portions of the descent trajectory.

In the subsequent discussion it will be convenient to let:

$$U(r) = \int_0^r N(r) dr = \bar{N} \int_0^r dr = \bar{N} r \quad (9)$$

where \bar{N} is the average density from 0 to r, i.e.

$$\bar{N} = \frac{1}{r} \int_0^r N(r) dr \quad (10)$$

We will now derive, for the case of horizontal stratification, the following useful relationship:

$$\frac{1}{r} \int_0^r N(r) dr = \frac{1}{z} \int_0^z N(z) dz \quad (11)$$

where $N(r)$ refers to the distribution along r and $N(z)$ refers to the distribution along z .

Horizontal stratification implies that the electron density is only a function of the altitude z . Thus the density N_j can be considered to be a constant within the thin horizontal lamination Δz_j shown in Fig. 3.

Equation (10) can be written

$$\bar{N} = \frac{1}{r} \lim_{\substack{k \rightarrow \infty \\ \Delta r \rightarrow 0}} \sum_{j=1}^{j=k} N_j \Delta r_j$$

$$\bar{N} = \frac{1}{r} \lim \sum N_j \Delta z_j / \cos \theta$$

$$\bar{N} = \frac{1}{r \cos \theta} \lim \sum N_j \Delta z_j$$

$$\bar{N} = \frac{1}{z} \int_0^z N dz \quad (12)$$

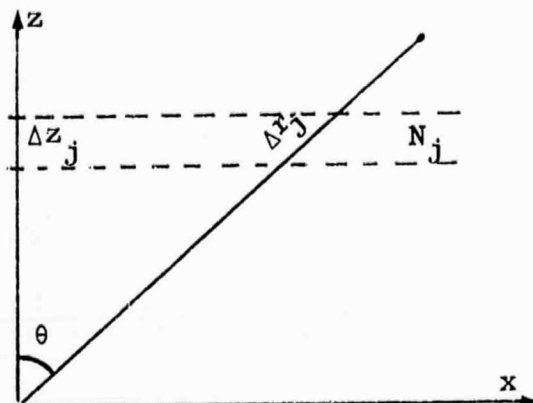


Fig. 3. Constant density lamination in a horizontally stratified ionosphere.

Theory of Experiment for Variable θ and Horizontal Stratification

The rocket is assumed to be travelling from A_1 to A_2 as indicated by Fig. 4. Let $r_1 = OA_1$ and $r_2 = OA_2$. The problem is to relate the density N in the height interval $z_2 - z_1$ to the measurement $U(r_2) - U(r_1)$.

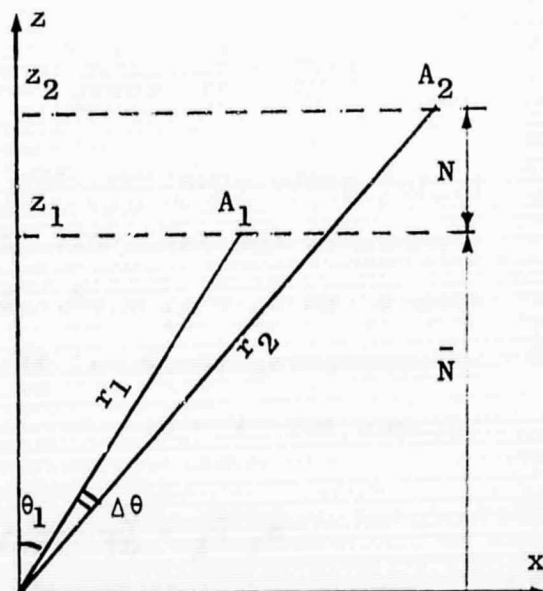


Fig. 4. Propagation paths for variable θ .

Since we have assumed horizontal stratification we can write for corresponding r and z :

$$\bar{N}(z) = \frac{1}{z} \int_0^z N dz = \frac{1}{r} \int_0^r N dr$$

Since $U(r) = \bar{N} r$ (see Eq. 9) we can write:

$$\begin{aligned} U(r) &= \frac{1}{z} \left(\int_0^z N dz \right) r \\ &= \frac{1}{\cos \theta} \int_0^z N dz \end{aligned}$$

$$U(r_2) - U(r_1) = \frac{1}{\cos \theta_2} \int_0^{z_2} N dz - \frac{1}{\cos \theta_1} \int_0^{z_1} N dz \quad (13)$$

Using Eq. (8) to express ΔU and letting $\int_0^{z_2} = \int_0^{z_1} + \int_{z_1}^{z_2}$ gives:

$$N' \Delta r = \left[\frac{1}{\cos \theta_2} - \frac{1}{\cos \theta_1} \right] \int_0^{z_1} N dz + \frac{1}{\cos \theta_2} \int_{z_1}^{z_2} N dz$$

or

$$N' \frac{\Delta r}{\Delta t} = \frac{1}{\Delta t} \left[\frac{1}{\cos \theta_2} - \frac{1}{\cos \theta_1} \right] \bar{N} z_1 + \frac{1}{\cos \theta_2} N \frac{\Delta z}{\Delta t}$$

In the above equation, the expression inside the bracket represents the increment of the function $1/\cos \theta$ as θ increases from θ_1 to $\theta_2 = \theta_1 + \Delta \theta$. Letting Δt be the time interval corresponding to $\Delta \theta$, it is seen that the above equation becomes for $\Delta t \rightarrow 0$:

$$\begin{aligned} N_1 \dot{r}_1 &= \frac{d}{dt} \left[\frac{1}{\cos \theta} \right]_{\theta=\theta_1} \bar{N}_1 z_1 + \frac{1}{\cos \theta_1} N_1 \dot{z}_1 \\ &= \left[\frac{(+\sin \theta) \dot{\theta}}{\cos^2 \theta} \right]_{\theta=\theta_1} \bar{N}_1 z_1 + \frac{1}{\cos \theta_1} N_1 \dot{z}_1 \end{aligned} \quad (14)$$

But

$$z = r \cos \theta$$

$$\dot{z}_1 = \dot{r}_1 \cos \theta_1 - r_1 (\sin \theta_1) \dot{\theta}_1$$

$$N'_1 \dot{r}_1 = r_1 (\tan \theta_1) \dot{\theta}_1 \bar{N}_1 + N_1 (\dot{r}_1 - r_1 (\tan \theta_1) \dot{\theta}_1)$$

and more generally (dropping the subscripts 1):

$$N' = \epsilon \bar{N} + N(1 - \epsilon) \quad (15)$$

where

$$\epsilon = \frac{r(\tan \theta) \dot{\theta}}{\dot{r}} \quad (16)$$

The approach used to derive Eq. (15) is based upon the geometrical interpretation of the measurement given by Fig. 4. A more formal procedure is to state that when $\Delta t \rightarrow 0$, we can write:

$$N' \dot{r} = \frac{d}{dt} U(z, \theta, t) = \frac{d}{dt} \left(\frac{1}{\cos \theta} \right) \int_0^z N dz \quad (17)$$

Keeping in mind that $\int_0^z N dz$ does not depend upon θ in this case, and expressing $\frac{d}{dt} U$ in terms of partial derivatives gives:

$$\begin{aligned} \frac{d}{dt} U &= \frac{\partial U}{\partial z} \frac{dz}{dt} + \frac{\partial U}{\partial \theta} \frac{d\theta}{dt} + \frac{\partial U}{\partial t} \frac{dt}{dt} \\ &= \dot{z} \left[\frac{\partial U}{\partial z} \right]_{\theta, t=\text{const}} + \dot{\theta} \left[\frac{\partial U}{\partial \theta} \right]_{z, t=\text{const}} + \left[\frac{\partial U}{\partial t} \right]_{z, \theta=\text{const}} \end{aligned}$$

The last term is zero for the horizontally stratified ionosphere (as defined earlier). Thus Eq. (17) becomes:

$$\begin{aligned}
N' \dot{r} &= \dot{z} \frac{1}{\cos \theta} \frac{\partial}{\partial z} \int_0^z N dz + \dot{\theta} \left(\int_0^z N dz \right) \frac{\partial}{\partial \theta} \frac{1}{\cos \theta} \\
&= \frac{N \dot{z}}{\cos \theta} + z \bar{N} \dot{\theta} \frac{\partial}{\partial \theta} \frac{1}{\cos \theta}
\end{aligned} \tag{18}$$

which is the same as Eq. (14).

A slightly more useful form of Eq. (15) is obtained as follows:

$$\begin{aligned}
N(1-\epsilon) &= N'(1-\epsilon) + \epsilon N' - \epsilon \bar{N} \\
&= N'(1-\epsilon) + \epsilon (N' - \bar{N})
\end{aligned}$$

$$\text{i.e.} \quad N = N' + \frac{\epsilon}{1-\epsilon} (N' - \bar{N}) \tag{19}$$

Equation (19) gives N in terms of N' , \bar{N} and a factor $\frac{\epsilon}{1-\epsilon}$ which depends only upon trajectory parameters (See Eq. 16).

It should be noted that \bar{N} is for the altitude z (i.e. for point A_1) and consequently it is known since the basic measurement provides $\bar{N} r_1$.

General Theory of the Experiment.

The derivation of Eq. (19) assumed that the electron density was a function of altitude only. This assumption is not made in the more general treatment which will now be given. The basic measurement technique, as illustrated by Fig. 4, yields for the height interval $z_2 - z_1$, the quantity:

$$U(r_2) - U(r_1) = \int_0^{r_2} N(r, t_2, \theta_2) dr - \int_0^{r_1} N(r, t_1, \theta_1) dr$$

where:

$N(r, t_2, \theta_2)$ is the electron density distribution along OA_2 (for $\theta = \theta_2$ and $t = t_2$), and

$N(r, t_1, \theta_1)$ is the electron density distribution along OA_1 (for $\theta = \theta_1$ and $t = t_1$)

The density at a given altitude Z is not necessarily the same for the two propagation paths, because $\theta_2 \neq \theta_1$ and because $t_2 \neq t_1$. The generalized expression for U must therefore include density variations due to t and θ , i.e.

$$U(r, t, \theta) = \int_0^r N(r, t, \theta) dr$$

The change of variable $z = r \cos \theta$ will be used to transform the expression $\int_0^r N(r, t, \theta) dr$, noting that t and θ are constants for the transformation. Thus

$$dz = dr \cos \theta$$

and

$$\int_0^r N(r, t, \theta) dr = \int_0^Z N(z, t, \theta) \frac{dz}{\cos \theta} = \frac{1}{\cos \theta} \int_0^Z N(z, t, \theta) dz \quad (20)$$

In Eq. (20), the quantities t and θ are functions of the upper limit of integration only. Furthermore $N(z, t, \theta)$ does not represent the vertical electron density distribution along the Z axis. The function $N(z, t, \theta)$ represents the distribution measured along a given path $OA = r$ for the corresponding values of t and θ .

Thus:

$$U(r, t, \theta) = \int_0^r N(r, t, \theta) dr = \frac{1}{\cos \theta} \int_0^z N(z, t, \theta) dz = U(z, t, \theta)$$

or

$$U(z, t, \theta) = \frac{z}{\cos \theta} \bar{N}(z, t, \theta) \quad (20a)$$

Since \bar{N} is now a function of θ and t , the partial derivations of U in Eq. (17) with respect to θ and t yield the following additional terms:

$$\frac{z}{\cos \theta} \frac{\partial \bar{N}}{\partial \theta} \quad \text{and} \quad \frac{z}{\cos \theta} \frac{\partial \bar{N}}{\partial t}$$

Letting $\frac{z}{\cos \theta} = r$ and recalling that $\frac{\partial U}{\partial \theta}$ is multiplied by $\dot{\theta}$ yields the following modified version of Eq. (15):

$$N' = \epsilon \bar{N} + N(1-\epsilon) + \frac{r}{\dot{r}} \left(\dot{\theta} \frac{\partial \bar{N}}{\partial \theta} + \frac{\partial \bar{N}}{\partial t} \right) \quad (21)$$

where $\frac{\partial \bar{N}}{\partial \theta}$ and $\frac{\partial \bar{N}}{\partial t}$ are for constant z .

Therefore Eq. (19) becomes:

$$N = N' + \frac{\epsilon}{1-\epsilon} (N' - \bar{N}) - \frac{r}{(1-\epsilon)\dot{r}} \left(\dot{\theta} \frac{\partial \bar{N}}{\partial \theta} + \frac{\partial \bar{N}}{\partial t} \right) \quad (22)$$

For very disturbed ionospheric conditions the error terms can be greater than N' , rendering the experimental measurement of N useless. For quiet and stable ionospheric conditions the error term is less than 5% for most of the ascent trajectory,

very large near apogee (where \dot{r} is very small), and 5 to 20% during descent. Some estimate of $\frac{\partial \bar{N}}{\partial t}$ for a quiet ionosphere can be derived from various measurements of the diurnal variation of \bar{N} (Ref. 7 and 8). These measurements provide \bar{N} for satellite-to-ground transmission paths and are therefore influenced primarily by the denser regions of the ionosphere at altitudes between 200 and 500 km. Assuming that $\partial \bar{N} / \partial t$ is proportional to \bar{N} and independent of the altitude range, the above measurements (Ref. 7 and 8) indicate that

$$\left| \frac{\partial \bar{N}}{\partial t} \right| < \frac{\bar{N}}{5000} \quad (\text{per second}) \quad (23)$$

Using the results of Little and Lawrence (Ref. 9), and making assumptions on $\partial \bar{N} / \partial \theta$ similar to those made on $\partial \bar{N} / \partial t$, one can arrive at the following upper estimate for $\frac{\partial \bar{N}}{\partial \theta}$:

$$\left| \frac{\partial \bar{N}}{\partial \theta} \right| < \frac{1}{2} \bar{N} \quad (\text{per radian}) \quad (24)$$

Thus $\left| \frac{\partial \bar{N}}{\partial t} \right| < q_1 \bar{N}$ and $\left| \frac{\partial \bar{N}}{\partial \theta} \right| < q_2 \bar{N}$

For undisturbed ionospheric conditions $q_1 = \frac{1}{5000}$ and $q_2 = \frac{1}{2}$. It is of interest to note that:

$$\frac{r}{(1-\epsilon)\dot{r}} = \frac{z}{\dot{z}} \quad (25)$$

which follows from $\dot{z} = \frac{d}{dt} (r \cos \theta) = \dot{r} \cos \theta - r(\sin \theta) \dot{\theta}$

$$\begin{aligned}\dot{z} &= (\cos \theta) [\dot{r} - r(\tan \theta) \dot{\theta}] \\ \dot{z} &= \dot{r}(\cos \theta) \left[1 - \frac{r}{\dot{r}}(\tan \theta) \dot{\theta}\right] \\ \dot{z} &= \dot{r}(\cos \theta) (1 - \epsilon)\end{aligned}\tag{26}$$

$$\frac{1}{\dot{r}(1-\epsilon)} = \frac{\cos \theta}{\dot{z}}$$

Thus the error term in Eq. (22) can be written:

$$\left| \frac{z}{\dot{z}} \left(\dot{\theta} \frac{\partial \bar{N}}{\partial \theta} + \frac{\partial \bar{N}}{\partial t} \right) \right| < \left| \frac{z}{\dot{z}} (\dot{\theta} q_2 + q_1) \bar{N} \right| \tag{27}$$

The only difference in ascent and descent errors (at equal altitudes) is due to $\dot{\theta}$, which is much greater for descent than for ascent.

Limiting Cases.

It is evident that Eq. (22) is not defined for either $\epsilon = 1$ or $\dot{r} = 0$. From the definition of ϵ (Eq. 16), it follows that $\epsilon = 1$ implies $\dot{r} = r(\tan \theta) \dot{\theta}$ and from Eq. (26) it is seen that $\dot{z} = 0$. Thus $\epsilon = 1$ corresponds to apogee when no measurement is made over a height Δz .

When $\dot{r} = 0$ we cannot define N' according to $\frac{dU}{dt} = N'\dot{r}$.

We can, however, write Eq. (14) as:

$$\begin{aligned}\frac{dU}{dt} &= r(\tan \theta) \dot{\theta} \bar{N} - N r(\tan \theta) \dot{\theta} \\ &= (\bar{N} - N) r(\tan \theta) \dot{\theta}\end{aligned}$$

which defines N in terms of \bar{N} . The above expression may not be very helpful if $\dot{r} = 0$ occurs very close to apogee, since \dot{z} would then be very small, causing the error term to become dominant.

SUMMARY

The experiment yields as a function of time, or equivalently $r(t)$:

$$U(r) = \int_0^r N(r) dr = \bar{N}r \quad (9)$$

The electron density N at $r(t_1)$, i.e. for $t = t_1$ is given by:

$$N = N' + \frac{\epsilon}{1-\epsilon} (N' - \bar{N}) \quad (19)$$

where

$$N' = \frac{1}{\dot{r}} \frac{d}{dt} U \quad \text{for } t = t_1$$

$$\epsilon = \frac{r(\tan\theta)\dot{\theta}}{\dot{r}} \quad \text{for } t = t_1 \quad (16)$$

$$\bar{N} = \frac{U}{r} \quad \text{for } t = t_1$$

The quantities r , \dot{r} , θ , $\dot{\theta}$, $\tan \theta$, are derived from the known rocket trajectory.

The error ΔN in the measurement is:

$$|\Delta N| < \left| \frac{Z}{\dot{z}} (|\dot{\theta}| q_2 + q_1) \bar{N} \right| \quad (27)$$

where (for undisturbed ionospheric conditions) we can let:

$$q_1 = \frac{1}{5000} \quad \text{and} \quad q_2 = \frac{1}{2} \quad (\dot{\theta} \text{ in radians/sec.})$$

TYPICAL RESULTS

The $N(h)$ profile shown by Fig. 5 was obtained under undisturbed ionospheric conditions ($K_p = 1$) with NASA 8.25 (peak altitude: 629 km) using the 24.5/73.6 MHz experiment. The $N(h)$ profile shown is based upon ascent data and it was calculated according to Eq. (19). The large irregularities ($\Delta N/N$) seen on the calculated topside profile are not consistent with typical topside sounder results which yield (particularly at midlatitudes) very smooth topside distributions. The $\Delta N/N$ fluctuations are consistent, however, with the errors indicated by Eq. (27). Using in Eq. (27) the values of q_1 and q_2 given for undisturbed ionospheric conditions yield the following expression for the maximum per cent error $\Delta N/N$:

$$\frac{\Delta N}{N} = \frac{z}{Z} \left(\frac{|\dot{\theta}|}{2} + \frac{1}{5000} \right) \frac{\bar{N}}{N} \quad (28)$$

The maximum error predicted by Eq. (28) is also shown (as a function of altitude) on Fig. 5. It is seen that the maximum amplitudes of the fluctuations on the calculated profile are very consistent with the curve showing $\frac{\Delta N}{N}$. Thus one would conclude that the $N(h)$ fluctuations are caused entirely by spatial and temporal variations along the propagation path.

The $N(h)$ profile shown by Fig. 6 was obtained during a disturbed period ($K_p = 4$) with NASA 18.98 (peak altitude: 295.1 km) using the 24.5/73.6 MHz experiment. The profile

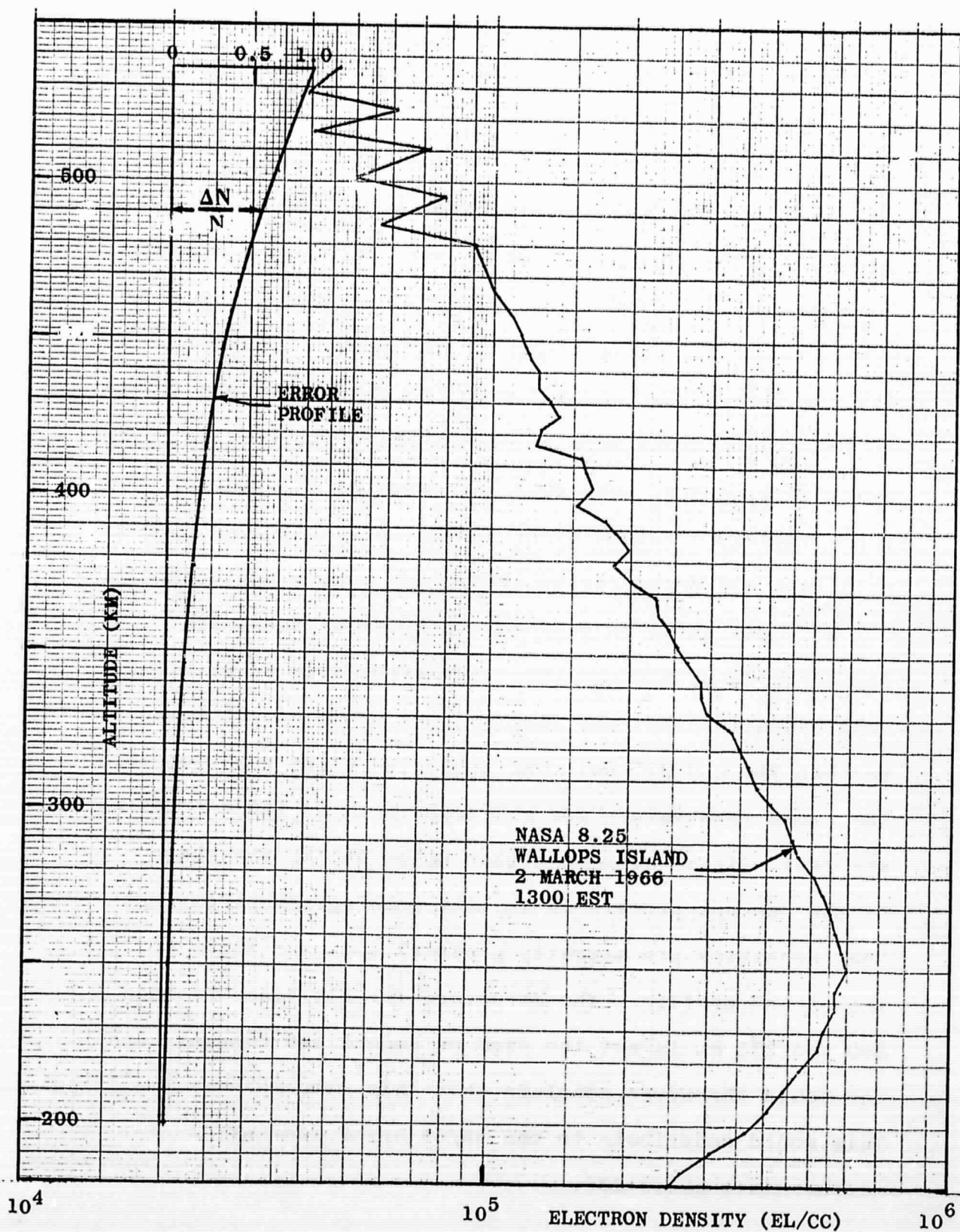


Fig. 5. Electron density profile and error profile for NASA 8.25

(solid curve for ascent and dashed curve for descent) was calculated according to Eq. (19). The calculations yielded a profile which was extremely smooth up to an altitude of 260 km and very irregular above 260 km. The error analysis can again be used to determine whether or not the structure is real. Since the measurements were made under disturbed ionospheric conditions, the values of q_1 and q_2 should be greater than the values used for the previous example. It was found that the computed error $\Delta N/N$ would be comparable to the fluctuations seen on ascent above 290 km (i.e. near peak) if q_1 and q_2 were both increased by a factor of 10. These increased values of q_1 and q_2 were therefore used to calculate the error curves (solid for ascent and dashed for descent) shown on Fig. 6. In spite of the large increases in q_1 and q_2 , the calculated error is significantly smaller than the fluctuations shown at altitudes between 260 and 275 km. One would therefore conclude that the large $\Delta N/N$ values for altitudes between 260 and 275 km are real. It is also seen that below 260 km the shape of the descent profile is in very good agreement (except that densities are slightly greater) with the shape of the ascent profile. The structure for altitudes between 260 and 275 km is not the same on ascent and descent, and one would therefore conclude that this structure is localized. This would contribute to the $\partial \bar{N} / \partial \theta$ error and influence measurements above 275.

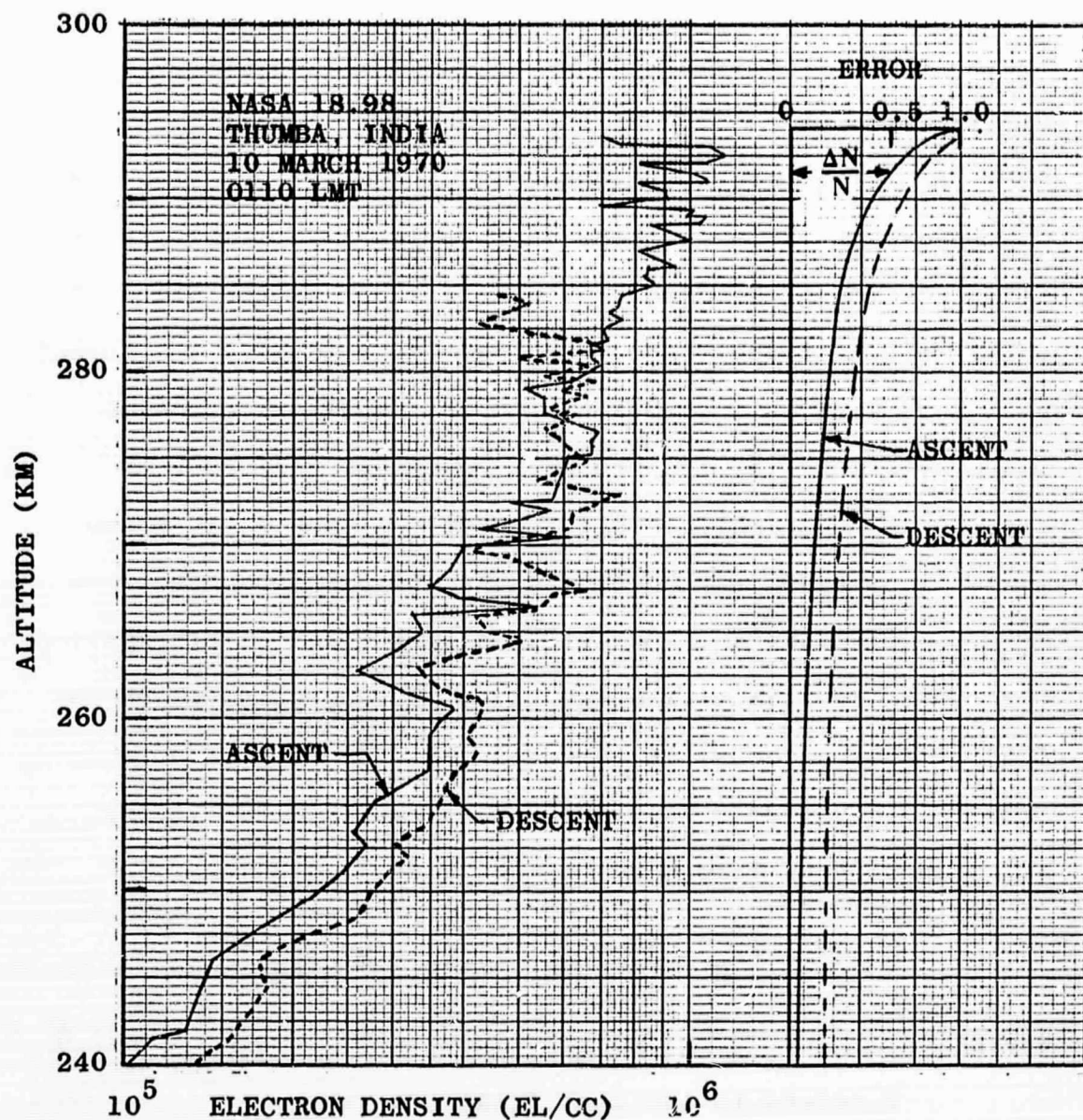


Fig. 6 Ascent and descent electron density profiles obtained with NASA 18.98, and corresponding error curves. The rocket was launched at 0130 IST (Indian Standard Time).

APPENDIX

Further Discussion of Measurement and Data Analysis Techniques

The treatment of the experiment given earlier has neglected phase shifts introduced by the rotation of the transmitting antennas on the spinning vehicle. A relatively high roll rate of several rotations per second is normally used on sounding rockets to maintain their dynamic stability at altitudes above the drag region. This causes the plane of polarization of the transmitted wave to rotate at the rocket roll rate, and this rotation produces equal and opposite phase shifts on the two propagation modes. In order to cancel the phase shift due to rocket roll the basic phase measurement $P_H - P_L$ represented by Eq. (5) is conducted with both the ordinary and the extraordinary modes of propagation (Ref. 2). The sum of the two phase measurements (which is free of roll effects) is taken as the basic measurement. Thus the actual 24.5/73.6 MHz experiment (Ref. 3) yields as a function of time a net phase shift Ψ_T given by:

$$\Psi_T = (\Psi_H - 3\Psi_L)_{\text{ORD.}} + (\Psi_H - 3\Psi_L)_{\text{EXT.}}$$

where:

H refers to the high frequency wave,

L refers to the low frequency wave,

ORD. refers to the ordinary mode of propagation,

EXT. refers to the extraordinary mode of propagation,

and the factor 3 is due to an effective frequency

multiplication by 3 of the received low frequency signal in order to compare its phase with the phase of the high frequency signal.

Expressing Ψ_T in terms of the refractive indices gives:

$$\Psi_T = \frac{f_H}{c} \int_0^r [(N_H - N_L)_{ORD} + (N_H - N_L)_{EXT}] dr$$

or

$$\Psi_T = \frac{f_H}{c} \int_0^r (S_n) dr \quad (29)$$

where $S_n = (N_H - N_L)_{ORD} + (N_H - N_L)_{EXT}$

For $f_H = 73.6$ MHz and $f_L = 24.5$ MHz, the quantity S_n is essentially independent of θ and B , and it is essentially a linear function of N , i.e.:

$$S_n = k N$$

Since k is not quite a constant, S_n will be written

$$S_n = \alpha k_o N \quad (30)$$

where:

$$k_o = 0.120,$$

N is in units of 10^6 el/cc, and

α is the function of αN shown in Fig. 7.

For the typical $N(h)$ profiles shown by Fig. 5 and 6, the electron density is less than 10^6 el/cc, and the value of α would be: $1.0 < \alpha < 1.04$. Thus no serious error would be introduced by letting $\alpha = 1.0$.

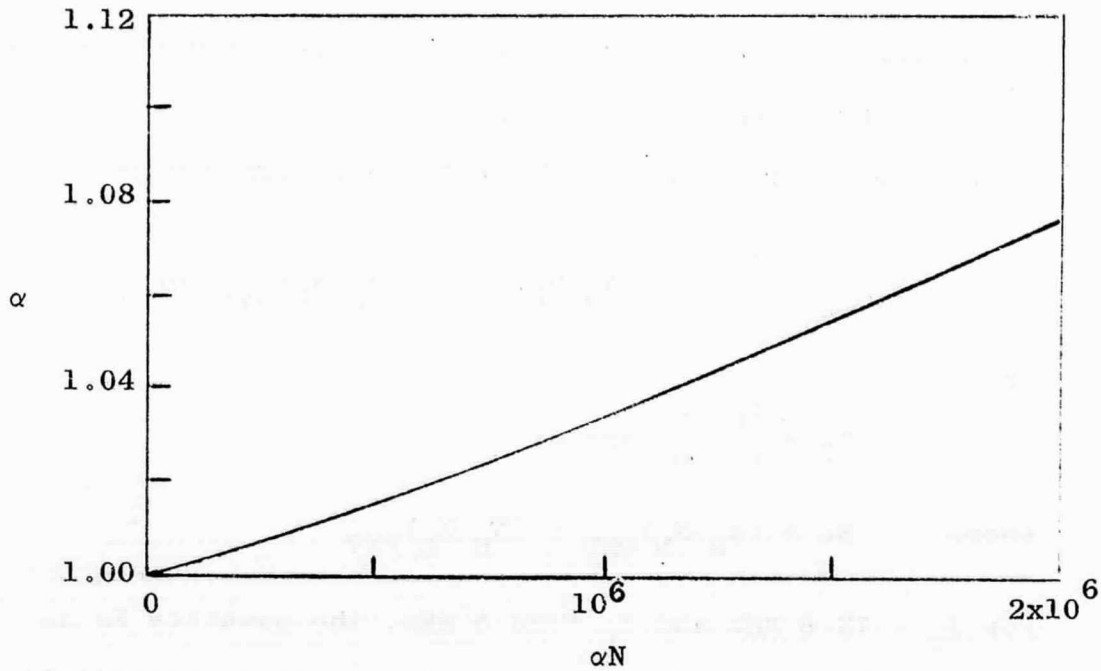


Fig. 7. The function α for $f_L = 24.5$ MHz and $f_H = 73.6$ MHz.

If desired a correction for α can be made as follows:

Substituting S_n from Eq. (30) into Eq. (29) yields:

$$\Psi_T = \frac{f_H}{c} k_O \int_0^r \alpha N dr$$

or

$$\int_0^r \alpha N dr = \frac{c \Psi_T}{f_H k_O}$$

In the earlier treatment the quantity U was used to represent $(c \Psi_T) / (f_H k_O)$. Retaining this definition of U , it is seen that:

$$U = \int_0^r \alpha N dr = \bar{\alpha} \bar{N} r$$

and

$$\frac{1}{r} = \frac{dU}{dt} = (\alpha N)_{\text{apparent}} = \alpha' N' \quad (31)$$

Thus the α correction consists simply in changing N to αN and it is readily seen that Eq. (19) would become:

$$\alpha N = \alpha' N' + \frac{\epsilon}{1-\epsilon} (\alpha' N' - \bar{\alpha} \bar{N}) \quad (32)$$

where

$$\begin{aligned} \alpha' N' &= \frac{1}{r} \frac{dU}{dt} = \frac{c \Psi_T}{r f_H k_O} \\ &= (3.40 \times 10^4) \dot{\Psi}_T / \dot{r} \quad (\dot{\Psi} \text{ in cycles/sec; } \dot{r} \text{ in km/sec}) \end{aligned}$$

$$\begin{aligned} \bar{\alpha} \bar{N} &= \frac{U}{r} = \frac{c \Psi_T}{r f_H k_O} \\ &= (3.40 \times 10^4) \Psi_T / r \quad (\Psi_T \text{ in cycles; } r \text{ in km}) \end{aligned}$$

The quantity αN given by Eq. (32) is converted to electron density using the appropriate value of α . The required value of α is found from Fig. 7 using the value of αN given by Eq. (32).

REFERENCES

1. Seddon, J.C., "Propagation Measurements in the Ionosphere with the Aid of Rockets", J. Geophys. Res., p. 323-335 (Sept. 1953).
2. Bauer, S.J. and J.E. Jackson, "A Small Multi-purpose Rocket Payload for Ionospheric Studies", NASA TN D-2323 (June 1964).
3. Bauer, S.J., L.J. Blumle, J.L. Donley, R.J. Fitzenreiter, and J.E. Jackson, "Simultaneous Rocket and Satellite Measurements of the Topside Ionosphere", J. Geophys. Res., p. 186-187 (1 Jan. 1964).
4. Goldberg, R.A. and L.J. Blumle, "Positive Ion Composition from a Rocket-borne Mass Spectrometer", J. Geophys. Res., p. 133-142 (1 Jan. 1970).
5. Aikin, A.C. and L.J. Blumle, "Rocket Measurements of the E-Region Electron Concentration Distribution in the Vicinity of the Geomagnetic Equator", J. Geophys. Res., p. 1617-1626 (1 March 1968).
6. Jackson, J.E., "Effect of Oblique Propagation Paths upon the NRL Rocket Studies of the Ionosphere", NRL Report 4960 (July 1957).
7. Garriott, O.K., F.L. Smith, and P.C. Yuen, "Observations of Ionospheric Electron Content Using a Geostationary Satellite", Planetary Space Science, p. 829-838, Vol. 13, 1965.

8. Titheridge, J.E., "Continuous Records of the Total Electron Content of the Ionosphere", J. Atmos. & Terrest. Phys., p. 1135-1150, Vol. 28, 1966.
9. Little, C.G. and R.S. Lawrence, "The Use of Polarization Fading of Satellite Signals to Study the Electron Content and Irregularities of the Ionosphere", J. Res. NBS 64D (Radio Prop.) p. 335, 1960.